Springer

KSME

Journal of Mechanical Science and Technology 29 (12) (2015) 5409~5416
www.springerlink.com/content/1738-494x(Print)/1976-3824(Online)
DOI 10.1007/s12206-015-1142-6

Coordinated control with electronic stability control and active steering devices †

Seongjin Yim*

Department of Mechanical and Automotive Engineering, Seoul National University of Science and Technology, 232 Gongneung-ro, Nowon-gu, Seoul, 139-743, Korea

(Manuscript Received July 21, 2014; Revised July 5, 2015; Accepted September 9, 2015)

Abstract

This paper presents a coordinated control with Electronic stability control (ESC), Active front steering (AFS) and Active rear steering (ARS). Direct yaw moment control is used to generate a control yaw moment. Weighted pseudo-inverse based control allocation (WPCA) is adopted to distribute the control yaw moment into tire forces, generated by ESC, AFS and ARS. Variable weights in WPCA are presented for several purposes. Simulations on vehicle simulation software, CarSim®, show that the proposed integrated chassis control is effective for maneuverability and lateral stability. Sensitivity analysis with Plackett-Burman method was done in order to check the effect of the variable weights.

Keywords: Active front steering (AFS); Active rear steering (ARS); Electronic stability control (ESC); Weighted pseudo-inverse based control allocation (WPCA)

1. Introduction

Before an Electronic stability control (ESC) was commercialized in middle of 1980s, 4-wheel steering (4WS) has been extensively studied for maneuverability and lateral stability since 1970s [1]. Most of the researches on 4WS have adopted a linear vehicle model, and feed-forward control for ARS. As a result, it was commercialized on passenger cars in 1980s. However, it had little effect on car market because of several drawbacks such as driver's discomfort, high maintenance cost, and large side-slip angle in transient stage.

Active front steering (AFS) was commercialized on passenger vehicles in middle of 2000s. AFS has the function of superposition angle in order to give a driver the steering comfort and active safety from variable steering gear ratio and active steering, respectively. Researches on AFS for vehicle stability control have been done in the several work [2, 3]. In these researches, the main function of AFS is to increase the vehicle speed in maintaining maneuverability and lateral stability. However, the use of AFS in under-steer situation is not effective because it did not reduce the vehicle speed.

Recently, 4WS with AFS and ARS was re-developed for passenger cars. Typical example is Nissan's 4-wheel active steer (4WAS), which consists of front and rear wheels controlled by Motor-driven power steering (MDPS) or Active front steering (AFS) and ARS, respectively [4]. Another examples are Delphi's Quadrasteer and BMW's Integral Active Steering. The lateral force of the front wheel is easily saturated when AFS is applied because AFS is added into the driver's steering. Compared to AFS, the most notable feature of ARS is that the lateral force of rear wheels is not saturated when ARS is applied.

Besides AFS and ARS, an ESC has been commercialized for maneuverability and lateral stability since 1980s. By virtue of the effectiveness of ESC in preventing vehicle crashes such as rollover and lost-of-control accidents, ESC installation on passenger vehicles has been mandatory since 2012 in USA [5]. However, the use of ESC makes a driver experience discomfort when it activated. This drawback of ESC can be overcome by using AFS or ARS.

ESC, AFS and ARS are complementary to each other. ESC is capable of reducing the vehicle speed, which is effective in under-steer situation. AFS and ARS can maintain the vehicle speed with steering comfort. Hence, the coordination between braking-based ESC and steering-based AFS and ARS can improve the ride comfort, maneuverability and lateral stability. To fully utilize the synergetic effects of ESC, AFS, and ARS, it is necessary to integrate these devices in a single framework. However, there have been little researches on integration of ESC, AFS and ARS to date. Integration schemes with ESC and AFS or ESC and ARS have been proposed [6, 7]. In the previous work, 4WS and ESC have been integrated by model following robust control [8]. In this research, a quadratic programming based control allocation, which requires a large amount of computation time, was adopted for yaw moment

*Corresponding author. Tel.: +82 2 970 9011, Fax.: +82 2 979 7032
E-mail address: acebtif@seoultech.ac.kr
† Recommended by Associate Editor Bongsob Song

distribution.

In this paper, coordinated control with ESC, AFS and ARS is investigated in order to improve the yaw rate tracking or maneuverability and the lateral stability. The controller has two-level structure: an upper-level and lower-level controller. In the upper-level controller, a direct yaw moment control is applied to generate a control yaw moment which is needed to stabilize a vehicle. In the lower-level controller, the control yaw moment is distributed with ESC, AFS and ARS using weighed pseudo-inverse based control allocation (WPCA). WPCA is a good candidate because it can solve the problem in real time through the algebraic computation [9-11]. To represent the actuator combination of ESC, AFS and ARS in WPCA framework, variable weights of the objective function in WPCA are proposed. To check the effectiveness of the proposed method for maneuverability and lateral stability, simulation is performed on a vehicle simulation package, CarSim® [12].

In the previous work [11], simulation-based tuning on the variable weights was adopted to optimize the variable weights. It was time-consuming and blind because there were no analyses on the effect of the variable weights. In this paper, sensitivity analysis with Plackett-Burman method, an experimental design method, is done in order to check the effects of the variable weights. From the analysis, it is shown how much a particular variable weight has an effect on the control performance.

This paper is organized as follows: In Sec. 2, a direct yaw moment controller is designed with a bicycle model, and yaw moment distribution schemes based on WPCA. In Sec. 3, simulation is conducted on Carsim. In Sec. 4, sensitivity analysis with Plackett-Burman method is done. The conclusions are given in Sec. 5.

2. Design of coordinated control with ESC, AFS and ARS

In this section, the coordinated controller with ESC, AFS, and ARS is designed. Direct yaw moment control and WPCA are adopted for control yaw moment generation and yaw moment distribution in the upper- and lower-level controllers, respectively. Variable weights in WPCA are defined for several objectives.

2.1 Design of an upper-level controller

The 2-DOF bicycle model is used to design a yaw moment controller. Fig. 1 shows the 2-DOF bicycle model. This model describes the yaw and the lateral motions of a vehicle, assuming that the longitudinal velocity v_x is constant.

The equations of motion for the 2-DOF bicycle model are obtained as follows:

$$\begin{aligned} mv_x\left(\dot{\beta}+\gamma\right) &= F_{yf}+F_{yr} \\ I_z\dot{\gamma} &= l_f F_{yf} - l_r F_{yr} + M_B \,. \end{aligned} \tag{1}$$

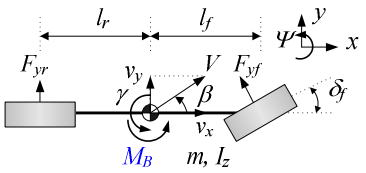

Fig. 1. 2-DOF bicycle model.

The reference yaw rate, generated by driver's steering input, can be algebraically calculated from the formula, given in Eq. (2), under the assumption that the lateral tire force is linear [13].

$$\gamma_d = \frac{C_f \cdot C_r \cdot \left(l_f + l_r\right) \cdot v_x}{C_f \cdot C_r \cdot \left(l_f + l_r\right)^2 + m \cdot v_x^2 \cdot \left(l_r \cdot C_r - l_f \cdot C_f\right)} \cdot \delta_f \,. \tag{2}$$

There are two typical objectives in vehicle stability control. The first is the maneuverability, which means the yaw rate tracking. The second is the lateral stability, which means the small side-slip angle. To improve these objectives, it is necessary for a yaw moment controller to make a vehicle follow the reference yaw rate and reduce the side-slip angle. To design a yaw moment controller, a sliding mode control is adopted in this paper. In order to achieve these objectives, the error surface is defined as Eq. (3). In Eq. (3), η is the parameter used to tune the trade-off between the yaw rate error and the side-slip angle. For the error surface to have a stable dynamics, the condition Eq. (4) should be satisfied [14].

$$s = \left(\gamma - \gamma_d\right) + \eta \cdot \beta \tag{3}$$

$$\dot{s} = -K_\gamma s \,. \tag{4}$$

By differentiating Eq. (3) and combining it with Eqs. (4) and (1), the control yaw moment M_B is obtained as Eq. (5).

$$\begin{aligned} M_B = {} & I_z \cdot \dot{\gamma}_d + I_z \cdot \eta \cdot \left(\frac{F_{yf} + F_{yr}}{m v_x} - \gamma \right) \\ & - l_f F_{yf} + l_r F_{yr} - I_z \cdot K_\gamma \cdot \left(\gamma - \gamma_d + \eta \cdot \beta\right) . \end{aligned} \tag{5}$$

2.2 Design of a lower-level controller

Once the control yaw moment M_B is computed in the upper-level controller, it should be distributed into braking forces of ESC and steering angles of AFS and ARS. In this paper, a WPCA is adopted to distribute the control yaw moment into the tire forces generated by ESC, AFS and ARS.

Fig. 2 shows the geometric relationship between the tire forces and the control yaw moment when the control yaw moment is positive. In Fig. 2, F_{x1}, F_{x2}, F_{x3} and F_{x4} are the longitudinal braking forces generated by ESC, and F_{yfc} and F_{yrc} are the lateral tire forces generated by AFS and ARS, respectively. These tire forces should be determined to generate the

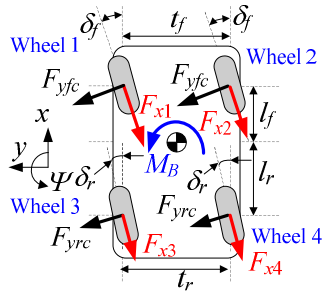

Fig. 2. Coordinate system corresponding to tire forces.

control yaw moment M_B. A WPCA is used to determine the tire forces [9].

Eq. (6) shows the geometric relation between the tire forces and control yaw moment, given in Fig. 2.

$$\underbrace{\begin{bmatrix} a_1 & a_2 & a_3 & a_4 & a_5 & a_6 \end{bmatrix}}_{\mathbf{H}} \underbrace{\begin{bmatrix} F_{yfc} \\ F_{yrc} \\ F_{x1} \\ F_{x2} \\ F_{x3} \\ F_{x4} \end{bmatrix}}_{\mathbf{q}} = M_B \tag{6}$$

$$a_1 = 2l_f \cos\delta_f, \quad a_2 = -2l_r \cos\delta_r$$

$$a_3 = -l_f \sin\delta_f + \frac{t_f}{2}\cos\delta_f, \quad a_4 = -l_f \sin\delta_f - \frac{t_f}{2}\cos\delta_f$$

$$a_5 = l_r \sin\delta_r + \frac{t_r}{2}\cos\delta_r, \quad a_6 = l_r \sin\delta_r - \frac{t_r}{2}\cos\delta_r .$$

The objective function of WPCA is defined as follows:

$$\begin{aligned} J &= \frac{\rho_1 F_{yfc}^2 + \rho_3 F_{x1}^2}{(\mu F_{z1})^2} + \frac{\rho_1 F_{yfc}^2 + \rho_4 F_{x2}^2}{(\mu F_{z2})^2} \\ &\quad + \frac{\rho_2 F_{yrc}^2 + \rho_5 F_{x3}^2}{(\mu F_{z3})^2} + \frac{\rho_2 F_{yrc}^2 + \rho_6 F_{x4}^2}{(\mu F_{z4})^2} \\ &= \mathbf{q}^T \mathbf{W} \mathbf{q} \end{aligned} \tag{7}$$

where $\mathbf{W} = diag\left[\frac{1}{\xi_1^2}+\frac{1}{\xi_2^2}, \frac{1}{\xi_3^2}+\frac{1}{\xi_4^2}, \frac{1}{\xi_1^2}, \frac{1}{\xi_2^2}, \frac{1}{\xi_3^2}, \frac{1}{\xi_4^2}\right]\boldsymbol{\rho}$, and $\boldsymbol{\rho} = [\rho_1\ \rho_2\ \rho_3\ \rho_4\ \rho_5\ \rho_6]^T$.

In Eq. (7), the vertical tire forces should be estimated because these cannot be easily measured. The vertical tire forces can be estimated with the longitudinal and lateral accelerations, as given in the previous work [7].

In Eq. (7), $\boldsymbol{\rho}$ is the vector of fictitious variable weights ρ_i. In this paper, $\boldsymbol{\rho}$ is used for several purposes [11]. Firstly, $\boldsymbol{\rho}$ is used to capture several actuator combinations such as ESC and ESC+AFS, ESC+ARS, ESC+AFS+ARS, and AFS+ARS. Secondly, $\boldsymbol{\rho}$ is used to limit excessive tire slip ratio and slip angle when ESC, AFS and ARS are applied. The detailed roles of $\boldsymbol{\rho}$ will be explained later.

The optimization problem is the quadratic programming with an equality constraint. Applying the Lagrange multiplier technique to this problem, the optimum solution can be easily obtained as Eq. (8). After obtaining the optimum solution $\mathbf{q}_{opt}$, each tire force is converted into the braking pressure P_B, active front steering angle $\Delta\delta_f$ and active rear steering angle δ_r as Eq. (8). In Eq. (9), F_{yfa} is the average of front lateral forces.

$$\mathbf{q}_{opt} = \mathbf{W}^{-1}\mathbf{H}^T\left(\mathbf{H}\mathbf{W}^{-1}\mathbf{H}^T\right)^{-1} M_B \tag{8}$$

$$\begin{cases} P_{Bi} = \dfrac{r_w}{K_B} F_{xi} \quad (i = 1,2,3,4) \\ \Delta\delta_f = \dfrac{F_{yfc} - F_{yfa}}{C_f} \quad for\ AFS \\ \delta_r = \dfrac{F_{yrc}}{C_r} \quad for\ ARS\ . \end{cases} \tag{9}$$

In this paper, five actuator combinations, ESC, ESC+AFS, ESC+ARS, ESC+AFS+ARS and AFS+ARS, are considered. For these actuator combinations, a particular constraint on yaw moment distribution is needed. For example, if only ESC is available and the control yaw moment is positive, then the longitudinal braking forces of left wheels, i.e,, F_{x1} and F_{x3} in Fig. 2, should be generated and those of right wheels, i.e,, F_{x2} and F_{x4}, should not be generated.

In order to capture these actuator combinations, the vector of variable weights $\boldsymbol{\rho}$ in Eq. (7) is introduced [11]. If the variable weight ρ_i in $\boldsymbol{\rho}$ is decreased, then the corresponding tire force F_{xi} or F_{yfc} or F_{yrc} is increased, and vice-versa. Using this fact, the distribution scheme can be set for each actuator combination. Let assume that all the variable weights in $\boldsymbol{\rho}$ are set to 1e-4. In this situation, if only ESC is available and the control yaw moment M_B is positive, the braking pressure can be applied to the left wheels. For this purpose, ρ_1, ρ_2 , ρ_4 and ρ_6 should be set to a high value, e.g., 1, as shown in Eq. (10). As a result of this setting, only F_{x1} and F_{x3} can be generated from WPCA. Following the fact, the sets of variable weights for each actuator combination can be determined as follows:

ESC

$$\begin{aligned} \boldsymbol{\rho} &= [1 \quad 1 \quad \varepsilon_1 \quad 1 \quad \varepsilon_2 \quad 1] \quad if\ M_B > 0 \\ \boldsymbol{\rho} &= [1 \quad 1 \quad 1 \quad \varepsilon_1 \quad 1 \quad \varepsilon_2] \quad if\ M_B < 0 \end{aligned} \tag{10}$$

ESC+AFS

$$\begin{aligned} \boldsymbol{\rho} &= [\varepsilon_1 \quad 1 \quad \varepsilon_2 \quad 1 \quad \varepsilon_3 \quad 1] \quad \text{if } M_B > 0 \\ \boldsymbol{\rho} &= [\varepsilon_1 \quad 1 \quad 1 \quad \varepsilon_2 \quad 1 \quad \varepsilon_3] \quad \text{if } M_B < 0 \end{aligned} \tag{11}$$

ESC+ARS

$$\begin{aligned} \boldsymbol{\rho} &= [1 \quad \varepsilon_1 \quad \varepsilon_2 \quad 1 \quad \varepsilon_3 \quad 1] \quad if\ M_B > 0 \\ \boldsymbol{\rho} &= [1 \quad \varepsilon_1 \quad 1 \quad \varepsilon_2 \quad 1 \quad \varepsilon_3] \quad if\ M_B < 0 \end{aligned} \tag{12}$$

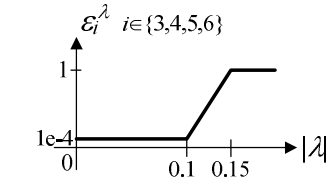

(a) Limit on variable weights for slip ratios

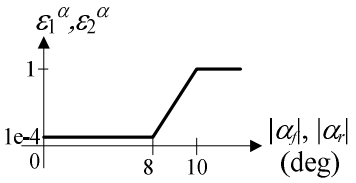

(b) Limit on variable weight for slip angles

Fig. 3. Limits on variable weights for limiting excessive slip ratio and slip angle.

ESC+AFS+ARS

$$\begin{aligned}\boldsymbol{\rho} &= \begin{bmatrix}\varepsilon_1 & \varepsilon_2 & \varepsilon_3 & 1 & \varepsilon_4 & 1\end{bmatrix} \quad if\ M_B > 0 \\ \boldsymbol{\rho} &= \begin{bmatrix}\varepsilon_1 & \varepsilon_2 & 1 & \varepsilon_3 & 1 & \varepsilon_4\end{bmatrix} \quad if\ M_B < 0\end{aligned} \tag{13}$$

AFS+ARS

$$\begin{aligned}\boldsymbol{\rho} &= \begin{bmatrix}\varepsilon_1 & \varepsilon_2 & 1 & 1 & 1 & 1\end{bmatrix} \quad if\ M_B > 0 \\ \boldsymbol{\rho} &= \begin{bmatrix}\varepsilon_1 & \varepsilon_2 & 1 & 1 & 1 & 1\end{bmatrix} \quad if\ M_B < 0\,.\end{aligned} \tag{14}$$

In the actuator configuration of ESC+AFS+ARS, the variable weights, ε_1, ε_2, ε_3 and ε_4, correspond to the use of AFS, ARS, and ESC on the front and rear wheels, respectively. If a particular variable weight increases, then the corresponding actuator will be less used. For instance, if ε_1 increases, lesser AFS will be used for yaw moment distribution. The effect of the variation of the variable weights will be investigated in Sec. 4.

2.3 Limit on variable weights for preventing saturation of the tire forces

Generally, the tire slip ratio is bounded by an Anti-lock braking system (ABS) because excessive tire slip ratio causes the saturation of the longitudinal tire force and the reduction of the lateral tire force. In this paper, the tire slip ratio and slip angles are regulated by limiting on the variable weights in yaw moment distribution stage. For this purpose, limits, ε_i^{λ}, on variable weights for F_{x1}, F_{x2}, F_{x3}, and F_{x4}, and limits, ε_1^{α} and ε_2^{α}, on variable weights for F_{yf} and F_{yr} are introduced to limit excessive tire slip ratios and slip angles, respectively. Figs. 3(a) and (b) show these limits on variable weights. With these limits, the variable weights ε_i from Eq. (10) to Eq. (14) are bounded by Eq. (15).

$$\begin{aligned}\rho_i &= \max\left\{\varepsilon_i, \varepsilon_i^{\alpha}\right\}, \quad i = 1,2 \\ \rho_i &= \max\left\{\varepsilon_i, \varepsilon_i^{\lambda}\right\}, \quad i = 3,4,5,6\,.\end{aligned} \tag{15}$$

Table 1. Parameters and values of a small-sized SUV model in CarSim.

m	1146.0 kg	I_z	1302.1 kg·m^2
C_f	36000 N/rad	C_r	50000 N/rad
l_f	0.88 m	l_r	1.32 m
v_x^i	80 km/h	r_w	0.398 m
$K_{B,front}$	150 N·m/MPa	$K_{B,rear}$	70 N·m/MPa

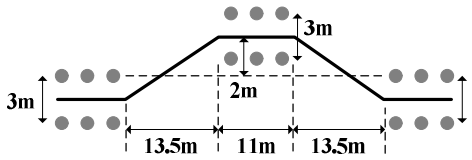

Fig. 4. Moose test track.

3. Simulation

In this section, simulations are performed to check the performance of the proposed method. Simulations are conducted for five actuator combinations, i.e., ESC, ESC+AFS, ESC+ARS, ESC+AFS+ARS, and AFS+ARS.

The simulation scenario is a closed-loop steering with a driver model. The simulation was performed on the vehicle simulation package, CarSim. The vehicle model used in simulation was the small-sized SUV model as provided by CarSim. Table 1 shows the parameters of the 2-DOF bicycle model, which were referred from the small-sized SUV model in CarSim. The path followed by the vehicle is the moose test track, as given in Fig. 4. The steering input is generated by the driver model, given in CarSim. The preview time of this driver model is set to 0.75 sec, which means an inexperienced driver [15]. The vehicle speed and the tire-road friction coefficient are set to 80 km/h and 0.6, respectively. The maximum AFS and ARS angles are bounded to 10 and 5 degrees, respectively. The actuators of the brake of ESC, AFS, and ARS were modeled as a first-order system with the time constants of 0.12, 0.05 and 0.05, respectively. ABS, provided in CarSim, is used to prevent the locking of a wheel in excessive braking.

Fig. 5 shows the simulation results for each actuator combination. Fig. 6 shows the applied braking pressures and AFS/ARS angles of the actuator combinations. In Fig. 6, the legends FL, FR, RL and RR represents the front left, front right, rear left and rear right wheels, respectively. In this paper, the yaw rate error or the maneuverability is regarded as satisfactory if it is less than 0.08 rad/s or 4.58 deg/s, as given by FMVSS 126, and the side-slip angle or the lateral stability is regarded as satisfactory if it is less than 3 deg [16].

As shown in Fig. 5, the uncontrolled vehicle was drifted because the tire-road friction coefficient is lower than that of dry asphalt. Contrary to this case, the controlled vehicles did not lose its stability. Coordinated control with all the actuator combinations gave satisfactory results in terms of the yaw rate

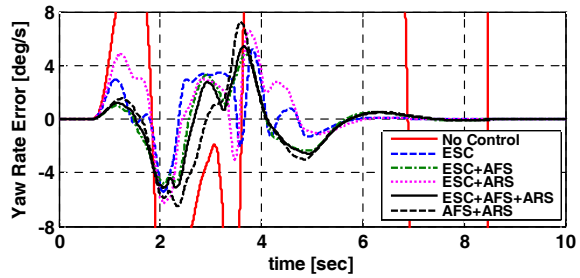

(a) Yaw rate error

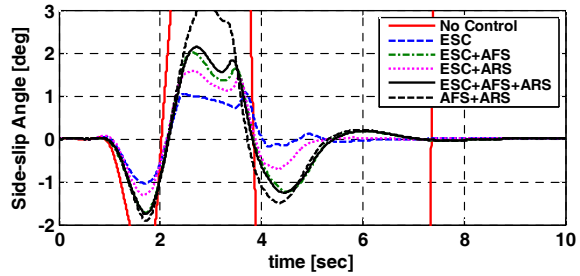

(b) Side-slip angle

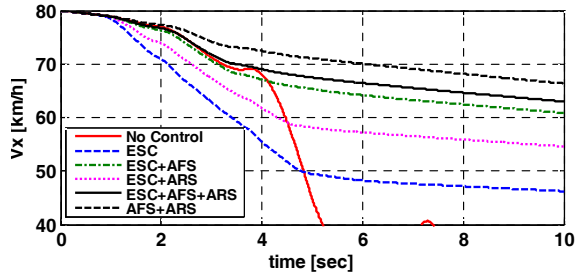

(c) Vehicle speed

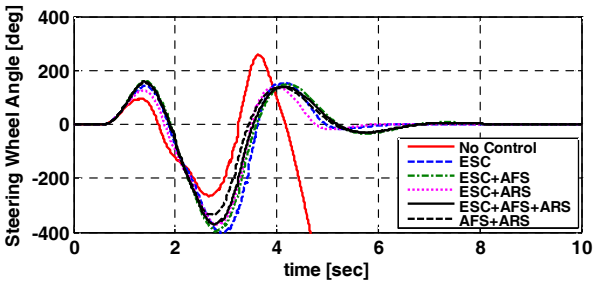

(d) Steering wheel angle

Fig. 5. Simulation results for each distribution scheme.

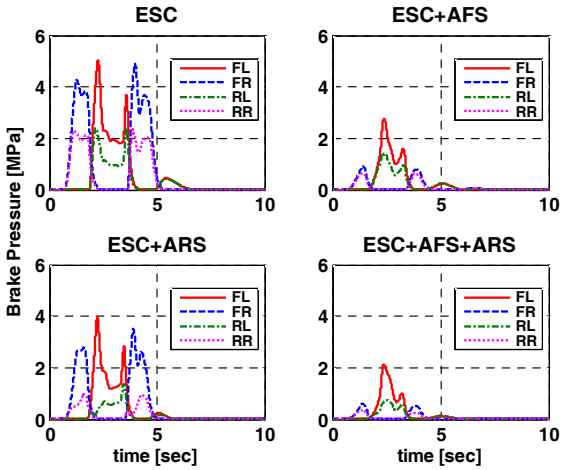

(a) Braking pressure for each actuator combination

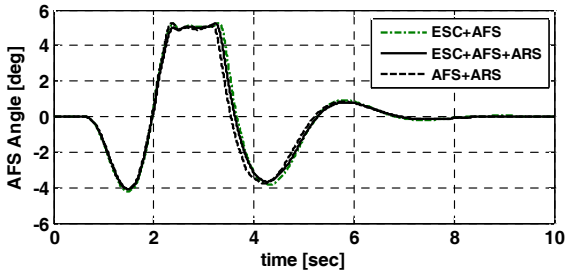

(b) AFS angle for each actuator combination

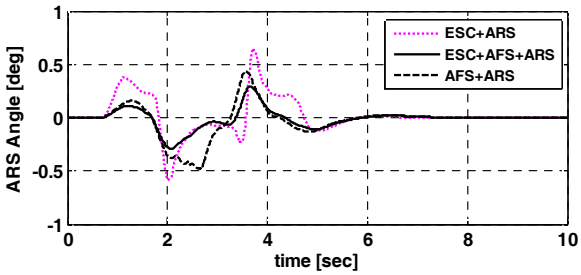

(c) ARS angle for each actuator combination

Fig. 6. Control inputs for each actuator combination.

error and side-slip angle. Every actuator combination has nearly identical steering wheel angles and yaw rate errors. However, the side-slip angles and vehicle speeds are different from one another. This is caused by the fact that the brake pressures of ESC+AFS and ESC+ARS are reduced, compared to those of ESC by virtue of AFS and ARS, as shown in Fig. 6(a). Moreover, it is shown that the effect of AFS is much larger than ARS in terms of brake pressure. As shown in Fig. 6(b), the steering angles of AFS are nearly identical although ARS is used. This means that the coordinated control with ESC, AFS, and ARS gives higher emphasis on AFS than ESC and ARS. As shown Figs. 5(a)-(c), the actuator combination of AFS+ARS gives the largest side-slip angle due to the maximum vehicle speed with the small yaw rate error. This is the typical drawback of 4WS.

Simulation results are summarized in Table 2. Table 2 shows the effects of actuator combinations on vehicle performance. As shown in Table 2, the maximum side-slip angle is proportional to the vehicle speed, and the vehicle speed is inversely proportional to the brake pressure. The actuator combination of AFS+ARS did not use the braking of ESC. As a result, it gave the largest vehicle speed and side-slip angle among others. For this reason, it is necessary to decrease the vehicle speed with the braking of ESC in order to reduce the side-slip angle.

Table 2. Effects of actuator combinations on vehicle performance.

Actuator combination	Maximum β	Final speed	Maximum P_B
ESC (only braking)	1.1 deg	46 km/h	5.0 MPa
ESC+AFS	2.0 deg	61 km/h	2.8 MPa
ESC+ARS	1.6 deg	55 km/h	4.0 MPa
ESC+AFS+ARS	2.1 deg	63 km/h	2.1 MPa
AFS+ARS (only steering)	3.2 deg	66 km/h	0 Mpa

Table 3. 8-experiment of 7 factors in PB method.

Experiment	Factors						
	ε_1	d_1	ε_2	d_2	ε_3	d_3	ε_4
1	+	–	–	+	–	+	+
2	+	+	–	–	+		+
3	+	+	+	–	–	+	–
4	–	+	+	+	–	–	+
5	+	–	+	+	+	–	–
6	–	+	–	+	+	+	–
7	–		+	–	+	+	+
8	–	–	–	–	–	–	–
Effect							
SS							
F-value							

4. Sensitivity analysis on the variable weights

In this section, the sensitivity analysis with Plackett-Burman (PB) method is done in order to check the effects of the variable weights. PB method has been widely used for screening factors that has little effect on outputs [17]. PB method makes use of two levels for each factor, the higher level (+) and the lower level (–), as given in Table 3. As shown in Table 3, four factors checked by PB method are ε_1, ε_2, ε_3 and ε_4 for ESC+AFS+ARS configuration. As mentioned in Sec. 2, the variable weights, ε_1, ε_2, ε_3 and ε_4, correspond to the use of AFS, ARS, and ESC on the front and rear wheels, respectively. In Table 3, d_1, d_2, and d_3 are dummy factors, which have no physical meaning. In this paper, the higher and lower levels of variable weights are set to 0.001 and 0.0001, respectively. In WPCA framework, the larger a particular variable weight, the smaller the corresponding tire force. For each experiment or a particular set of variable weights in Table 3, simulation is performed on CarSim under the identical conditions as given in Sec. 3. Outputs of each experiment are the yaw rate error, the side-slip angle, and the final vehicle speed.

The effect of a factor is calculated as Eq. (16). In Eq. (16), N is the number of experiments. (+) and (-) represent the outputs of a given factor at its higher and lower levels, respectively. For analysis of variance (ANOVA), the sum of squares (SS) is calculated as Eq. (17). F-value of each factor is calculated by dividing its SS by the sum of SS's of dummy factors. The critical value of $F_{1,3}$ at $p = 0.05$ is 10.13.

Table 4. Result of PB method for the yaw rate error (deg/s).

	Factors			
	ε_1	ε_2	ε_3	ε_4
Effect	-0.4200	-0.7600	0.8400	0.6550
SS	0.3528	1.1552	1.4112	0.8580
F-value	4.0351	13.2124	16.1403	9.8138

Table 5. Result of PB method for the side-slip angle (deg).

	Factors			
	ε_1	ε_2	ε_3	ε_4
Effect	-0.3625	-0.2075	0.6825	0.2575
SS	0.2628	0.0861	0.9316	0.1326
F-value	106.00	34.734	375.77	53.491

Table 6. Result of PB method for the final speed (km/h).

Experiment	Factors			
	ε_1	ε_2	ε_3	ε_4
Effect	-3.0000	-3.6500	2.4500	3.0000
SS	18.000	26.645	12.005	18.000
F-value	63.905	94.597	42.621	63.905

So, the change of a particular factor is significant if F-value of the corresponding factor is larger than 10.13.

$$Effect = 2\left\{\sum(+) - \sum(-)\right\}/N \tag{16}$$

$$SS = N \times (Effect)^2 / 4 . \tag{17}$$

Tables 4-6 show the results of PB method for yaw rate error, side-slip angle and final speed. In these tables, a negative effect means that the output decreases if the corresponding factor or variable weight increases. As shown in Table 4, the most effective variable weight for yaw rate error reduction is ε_3, which means that the smaller use of ESC on the front wheels makes the yaw rate error increased. On the other hand, ε_2 (ARS) and ε_4 (ESC on the rear wheels) have also a large effect on the yaw rate error. If ε_3 and ε_4 are increased or lesser ESC is used, the yaw rate error increases because the vehicle speed is fast. As shown in Tables 4 and 5, the variable weight ε_3 or ESC on the front wheels has the largest effect on the yaw rate error and side-slip angle. This results from the fact that the use of ESC makes the controlled vehicle slow. As shown in Table 6, the variable weight ε_2 or ARS has the largest effect on the final vehicle speed. Moreover, ε_1 (AFS) and ε_4 (ESC on the rear wheels) have also a large effect on the final vehicle speed. From these results, it can be known that lesser use of ESC makes the controlled vehicle fast.

As shown in Tables 4-6, this tendency of the effects of variable weights to the yaw rate error is identical to those of PB

method for side-slip angle. In other words, the increase of ε_1 and ε_2 has the negative effect on the outputs. Moreover, the increase of ε_3 and ε_4 has the positive effect on the outputs. From these results, it can be concluded that it is essential to use ESC with differential braking for reduction of yaw rate error and side-slip angle.

5. Conclusion

In this paper, the coordinated control with ESC, AFS and ARS was proposed. For the coordinated control, the WPCA was adopted to coordinate several actuator combinations, ESC, ESC+AFS, ESC+ARS, ESC+AFS+ ARS, and AFS+ARS. To use the WPCA for yaw moment distribution, variable weighs corresponding to the actuator combination were proposed. Through simulations, it was shown that the proposed coordinated control with ESC, AFS, and ARS is satisfactory for yaw moment control. It was shown that AFS is dominant for reducing the brake pressure of ESC, and that the actuator combination of AFS and ARS can generate a larger side-slip angle due to the lack of braking in ESC. It was also shown that the braking of ESC is necessary to use in order to reduce the side-slip angle. Sensitivity analysis with Plackett-Burman method was done to check the effect of the variable weights.

Acknowledgment

This study was supported by Seoul National University of Science and Technology.

Nomenclature

a_x, a_y : Longitudinal and lateral accelerations (m/s^2)
C_f, C_r : Cornering stiffness of front/rear tires (N/rad)
F_{yf}, F_{yr} : Lateral tire forces of front and rear wheels (N)
F_{yrf}, F_{yrc} : Lateral tire force generated by AFS and ARS(N)
g : Gravitational constant (= 9.81 m/s^2)
H : Effectiveness matrix in WPCA
I_z : Yaw moment of inertial (kg·m^2)
K_γ : DYC gain in sliding mode control
K_B : Pressure-force constant (N·m/MPa)
l_f, l_r : Distance from C.G. to front and rear axles (m)
m : Vehicle total mass (kg)
M_B : Control yaw moment (Nm)
P_B : Brake pressure (MPa)
q : Vector of tire forces
r_w : Radius of a wheel (m)
SS : The sum of squares on outputs of each factor
t_f, t_r : Track width of front and rear axles (m)
v_x, v_y : Longitudinal and lateral velocities of a vehicle (m/s)
V : Vehicle speed (m/s)
W : Weighting matrix in WPCA
α_f, α_r : Tire slip angles of front and rear wheels (rad)
β : Side-slip angle (rad)
ε : Weight for a particular tire force
δ_f, δ_r : Front and rear steering angles (rad)
$\Delta\delta_f$: Active front steering angle (rad)
γ, γ_d : Real and reference yaw rates (rad/s)
η : Tuning parameters on yaw rate error and side-slip angle
μ : Tire-road friction coefficient
$\boldsymbol{\rho}$: Vector of variable weights in WPCA

References

[1] Y. Furukawa, N. Yuhara, S. Sano, H. Takeda and Y. Matsushita, A review of four-wheel steering studies from the viewpoint of vehicle dynamics and control, *Vehicle System Dynamics*, 18 (1989) 151-186.
[2] M. Nagai, M. Shino and F. Gao, Study on integrated control of active front steer angle and direct yaw moment, *JSAE Review*, 23 (2002) 309-315.
[3] B. S. Caglar, K. I. Emre and A. Gunay, Handling stability improvement through robust active front steering and active differential control, *Vehicle System Dynamics*, 49 (5) (2011) 657-683.
[4] Nissan Motor Company, 4 Wheel Active Steer (4WAS), *www.nissan-global.com/EN* (2006).
[5] National Highway Traffic Safety Administration, Federal motor vehicle safety standards; electronic stability control systems; controls and displays, *NHTSA-2007-27622* (2007).
[6] M. Nagai, Y. Hirano and S. Yamanaka, Integrated control of active rear wheel steering and direct yaw moment control, *Vehicle System Dynamics*, 27 (5-6) (1997) 357-370.
[7] W. Cho, J. Yoon, J. Kim, J. Hur and K. Yi, An investigation into unified chassis control scheme for optimised vehicle stability and maneuverability, *Vehicle System Dynamics*, 46 Supplement, (2008) 87-105.
[8] S. Yoo, S. H. You, J. Jo, D. Kim and K. I. Lee, Optimal integration of active 4-wheel steering and direct yaw moment control, *11th IFAC Symposium on Control in Transportation Systems* (2006) 603-608.
[9] J. Wang and R. G. Longoria, Coordinated vehicle dynamics control with control distribution, *Proceedings of the 2006 American Control Conference*, Minneapolis, Minnesota, USA (2006) 5348-5353.
[10] N. Ando and H. Fujimoto, Yaw-rate control for electric vehicle with active front/rear steering and driving/braking force distribution of rear wheels, *11th IEEE International Workshop on Advanced Motion Control*, Nagaoka, Japan (2010) 726-731.
[11] S. Yim, J. Choi and K. Yi, Coordinated control of hybrid 4WD vehicles for enhanced maneuverability and lateral stability, *IEEE Transactions on Vehicular Technology*, 61 (4) (2012) 1946-1950.
[12] Mechanical Simulation Corporation, *CarSim User Manual Version 5* (2001).
[13] R. Rajamani, *Vehicle Dynamics and Control*, New York, Springer (2006).
[14] K. Uematsu and J. C. Gerdes, A comparison of several

sliding surfaces for stability control, *7th IEEE International Workshop on Advanced Motion Control*, Hiroshima, Japan (2002).

[15] C. C. MacAdam, Application of an optimal preview control for simulation of closed-loop automobile driving, *IEEE Transactions on Systems, Man, and Cybernetics*, 11 (6) (1981) 393-399.

[16] National Highway Traffic Safety Administration, *FMVSS No. 126, Electronic Stability Control Systems, NHTSA Final Regulatory Impact Analysis* (2007).

[17] Analytical Methods Committee, AMCTB No 55, Experimental design and optimisation (4): Plackett-Burman designs, *Analytical Methods*, 5 (2013) 1901-1903.

Seongjin Yim received the B.S. degree in mechanical engineering from Yonsei University, Korea, in 1995, and the M.S. and Ph.D. degrees in mechanical engineering from the Korea Advanced Institute of Science and Technology (KAIST) in 1997 and 2007, respectively. From 2011 to 2012, he has been a research professor in Advanced Institutes of Convergence Technology, Korea. Since 2013, he has been an assistant professor in Seoul National University of Science and Technology. His research interests are robust control, vehicle rollover prevention, and integrated chassis control systems.